

pubs.acs.org/JCTC Letter

An Accurate Density Coherence Functional for Hybrid Multiconfiguration Density Coherence Functional Theory

Dayou Zhang and Donald G. Truhlar*



Cite This: J. Chem. Theory Comput. 2023, 19, 6551-6556



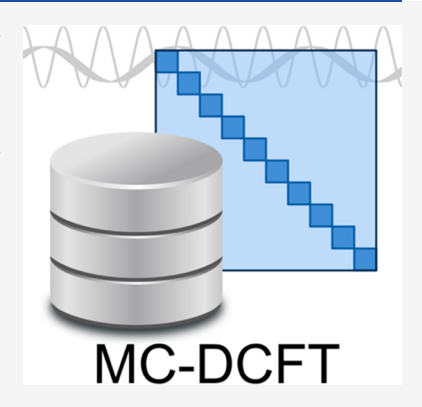
ACCESS I

III Metrics & More

Article Recommendations

SI Supporting Information

ABSTRACT: We present hybrid multiconfiguration density coherence functional theory (HMC-DCFT), and we optimize a density coherence functional by parametrization against a diverse data set of 59 bond energies and 60 barrier heights. We compare the results to calculations on the same data set by CASSCF, CASPT2, six Kohn—Sham and hybrid Kohn—Sham exchange—correlation functionals, and three on-top functionals for pair-density functional theory (PDFT) and hybrid PDFT. The new functional has better accuracy than all compared methods.



E lectronic structure calculations with a multiconfiguration reference wave function are useful tools for calculations on systems with strong static correlation because of their inherently multiconfigurational nature. 1-30 One usually carries out such calculations in two steps. Typically one starts with a multiconfigurational self-consistent-field (MCSCF) wave function, such as a complete active space self-consistent-field (CASSCF)^{31,32} wave function or a density matrix renormalization group self-consistent field (DMRG-SCF)^{33,34} wave function, or with a valence bond¹⁵ wave function, followed by perturbation theory^{2,4,15,35} or multireference configuration interaction (MRCI).^{1,5,7,13,17} The first step should recover the static correlation energy, and inevitably, it will also recover some of the dynamic correlation energy; in the second step, called a multireference step since it starts out with a multiconfiguration wave function as the reference function, one attempts a more complete calculation that includes the rest of the dynamic correlation energy. The second step is often the more computationally expensive step, especially for larger systems. The large computational cost for quantitatively accurate wave function calculations with multireference methods often makes their cost prohibitive. This provides strong motivation to develop inexpensive alternative post-MCSCF methods while still retaining high accuracy.

One possible way to make post-MCSCF calculations more affordable is to combine multiconfiguration wave functions with density functional theory. This has been proposed by many authors (we gave 44 references in our original paper³⁶ on this subject), and we cite multiconfiguration pair-density functional theory (MC-PDFT)^{36,37} as an example that has proved successful and that serves as an especially relevant

background to the present paper. A generalization of MC-PDFT is multiconfiguration nonclassical functional theory (MC-NEFT). MC-NEFT calculates the total electronic energy by separately evaluating a classical energy, $E_{\rm class}$, and a nonclassical energy, $E_{\rm nc}$.

$$E_{\text{MC-NEFT}} = E_{\text{class}} + E_{\text{nc}} \tag{1}$$

The classical energy, E_{class} , which includes electronic kinetic energy, electron-nuclear attraction, classical electron-electron electrostatics, and nuclear-nuclear repulsion, is evaluated conventionally from a multiconfigurational wave function. The nonclassical energy, E_{nc} , is approximated using a functional called a nonclassical energy functional, which is a functional of some properties (called ingredients) of the multiconfigurational wave function. An especially important difference between Kohn-Sham DFT40 (KS-DFT) and MC-NEFT is the way they treat intrinsically multiconfigurational hyper-open open-shell systems (for example, highly stretched single bonds and other open-shell singlets or doublets with three unpaired electrons). In the way it is usually employed,⁴¹ KS-DFT treats these with a broken-symmetry Slater determinant that has unphysical magnetization density, whereas MC-NEFT gives a physical description of the static correlation, prompting the expectation that one can use the

Received: July 5, 2023

Published: September 14, 2023





ingredients of the multiconfiguration wave function to obtain systematically more accurate descriptions of intrinsically multiconfigurational systems. We elucidated one of the reasons why MC-NEFT works well by an energy decomposition study.⁴²

The original MC-NEFT was MC-PDFT, 36,37 in which the ingredients in the energy functional are the density $\rho(\mathbf{r})$, which is the diagonal element of the 1-particle reduced density matrix (1-RDM) in the coordinate representation, and the on-top pair density $\Pi(\mathbf{r})$, which is the fully diagonal element of the two-particle reduced density matrix (2-RDM) in the coordinate representation. The resulting nonclassical energy functionals are called on-top functionals. MC-PDFT has been found to have good accuracy systems with strong static correlation. $^{23,43-45}$

We also developed a hybrid version⁴⁶ of MC-PDFT, in which the nonclassical energy functional is constructed by mixing a portion of the MCSCF exchange—correlation energy, $E_{\rm MC,XC}$, with the on-top energy, $E_{\rm OT}$

$$E_{\text{HMC-PDFT}} = E_{\text{class}} + XE_{\text{MC,XC}} + (1 - X)E_{\text{OT}}$$
 (2)

where X is a parameter, and $E_{\rm OT}$ is the nonclassical energy evaluated from the on-top functional. The hybrid MC-NEFT based on the MC-PDFT framework is called HMC-PDFT, ⁴⁶ and it has shown improved accuracy over the straight MC-PDFT method. ^{44,46–48}

Another example of MC-NEFT used machine-learned nonclassical functionals based on MC-PDFT, and the resulting theory was called a multiconfiguration data-driven functional method (MC-DDFM);³⁸ this showed promising results for predicting excitation energies.

Multiconfiguration density coherence functional theory (MC-DCFT)³⁹ provides another way to carry out MC-NEFT. It not only uses the density $\rho(\mathbf{r})$ but also uses the density coherences $\rho(\mathbf{r}|\mathbf{r}')$, which are the off-diagonal elements of the 1-RDM in the coordinate representation, to construct the nonclassical energy functional. This is motivated by the close connection between the unpaired electron density and the density coherences. ^{29,39,49–51} In our initial exploration of MC-DCFT, we used density coherence functionals converted directly from KS-DFT exchange—correlation functionals, and we found that they have a systematic error due in part to the quantitative differences between the unpaired-electron densities and the needed effective spin densities; we also found that the systematic error can be reduced by reparametrizing the density coherence functional.

In the present work, we explore the question of whether we can optimize a multiconfiguration nonclassical energy functional by methods that have been successful for single-configuration KS-DFT. We do this in the context of a hybrid version of MC-DCFT, which will be called HMC-DCFT. In HMC-DCFT, we have (as in eq 2)

$$E_{\text{HMC-DCFT}} = E_{\text{class}} + XE_{\text{MC,XC}} + (1 - X)E_{\text{DC}}$$
(3)

The density coherence functionals for the present study are written as functions of the unpaired densities defined by $^{49-51}$

$$D(\mathbf{r}) = 2\rho(\mathbf{r}) - \int [\rho(\mathbf{r}|\mathbf{r}')]^2 d\mathbf{r}'$$

$$= \sum_{i} n_i (2 - n_i) \chi_i^2(\mathbf{r})$$
(4)

where n_i is the occupation number of natural orbital i, and $\chi_i(\mathbf{r})$ is the magnitude of natural orbital i in the MCSCF reference wave function. To obtain a functional form, we convert a KS exchange-correlation functional, which is a functional depending on effective spin densities $\tilde{\rho}_{\alpha}(\mathbf{r})$ and $\tilde{\rho}_{\beta}(\mathbf{r})$, by using

$$\tilde{\rho}_{\alpha}(\mathbf{r}) = \frac{1}{2}\rho(\mathbf{r}) + \frac{1}{2}D(\mathbf{r}) \tag{5}$$

$$\tilde{\rho}_{\beta}(\mathbf{r}) = \frac{1}{2}\rho(\mathbf{r}) + \frac{1}{2}D(\mathbf{r}) \tag{6}$$

Once we obtain the effective spin densities and their gradients using eqs 4–6, we use the KS-DFT functional to evaluate the nonclassical energy, $E_{\rm nc}$. In the context of HMC-DCFT, this becomes $E_{\rm DC}$ in eq 3. There are two qualitative differences between on-top functionals (giving the energy $E_{\rm OT}$) and a density coherence functional (giving the energy $E_{\rm DC}$). First, in an on-top functional, the nonclassical energy density at a point ${\bf r}$ in space depends only on properties $[\rho({\bf r})$ and $\Pi({\bf r})]$ at that point in space, whereas the density coherence is nonlocal, depending on ${\bf r}'$ as well as ${\bf r}$. Second, $E_{\rm OT}$ depends on both 1-RDM and 2-RDM, whereas $E_{\rm DC}$ depends only on the 1-RDM.

In this work, we used a CASSCF reference function. To systematically develop or test a nonclassical energy functional, we need a systematic method of selecting the active space that minimizes the need for nonsystematic judgment. We therefore used a systematic scheme to generate active spaces, and it is described in the Supporting Information (SI), which also gives the other computational details. Default initial guesses of standard software are used for all CASSCF calculations, with point group symmetry disabled. To minimize human judgment in the entire computation, we did not attempt to achieve better results by manually adjusting the initial guess orbitals or the active space; we used the initial guesses provided by OpenMolcas⁵² for one data set and Molpro⁵³⁻⁵⁵ for another data set, and we used active spaces generated by the systematic scheme. Prior to filtering (the filtering step is explained below), the molecules and geometries are the same in both data sets, but the initial guess orbitals and SCF algorithms are different.

We constructed the two data sets from diatomic dissociation energies in ref 56, from diatomic and polyatomic bond dissociation energies in data sets MR-MGM-BE4, MR-MGN-BE17, MR-TM-BE12, SR-MGM-BE8, SR-MGN-BE107, and SR-TM-BE15 in Minnesota Database 2019⁵⁷ (we excluded atomization energies that involve dissociation of more than one bond) and from the HTBH38 and NHTBH38 reaction barrier height data sets of Minnesota Database 2019. Since all electronic structure calculations in this study are without spin—orbit coupling, we added experimental spin—orbit contributions when nonzero.

Bond dissociation energies are calculated by stretching a bond to 8 Å. The calculation of a bond dissociation energy or barrier height is a difference ΔE of two energies (stretched molecule relative to equilibrium molecule or transition state relative to reactants or products), and it therefore requires two CASSCF calculations to generate the reference wave functions. For developing and testing density functionals, we want to use only calculations for which the CASSCF wave functions are good zero-order wave functions (i.e., are based on good active spaces) for the ΔE under consideration, so that the errors are a measure of the quality of the density functional with a reasonable active space rather than a measure of errors due to a poor active space. Therefore, because the automatic active

space scheme explained in the SI does not always produce a good active space, we need to limit the calculations to those cases where it does produce a good active space. A good active space should yield a CASPT2 energy that is not too far from the accurate one, and it should not lead to too large of a difference between the CASSCF and CASPT2 energies. To reflect this, our criterion for a good active space for a bond energy or barrier height is that both of the following inequalities are satisfied:

$$|\Delta E(\text{CASSCF}) - \Delta E(\text{CASPT2})| < 1.1 \text{ eV } (25.4 \text{ kcal/mol})$$
(7)

$$|\Delta E(CASPT2) - \Delta E(accurate)| < 0.4 \text{ eV } (9.2 \text{ kcal/mol})$$
 (8)

The first inequality ensures that the energy difference at the CASPT2 level does not deviate from CASSCF by a large amount, while the second inequality (eq 8) ensures that CASPT2 is able to accurately predict the energy difference. The values of the parameters in both inequalities are based on our experience with active space selection. We also excluded active spaces for which a CASSCF or CASPT2 calculation did not converge, and to reduce the computational effort of the calculations, we also excluded active spaces larger than 12 electrons in 12 orbitals. After these filtering criteria, we have 119 accurate bond-energy or barrier-height active spaces, of which 54 come from Molpro calculations (we refer to them as Data Set 1 (DS1)) and 65 come from OpenMolcas calculations (we refer to them as Data Set 2 (DS2)). Using the filtered active spaces, DS1 has 27 bond energies and 27 barrier heights, and DS2 has 32 bond energies and 33 barrier heights. The data in these data sets are diverse, including both main-group and transition-metal data (full details of the data sets are in Table S2 of the SI).

We used the same functional form as the B97 and HCTH series⁵⁸⁻⁶⁰ of KS-DFT functionals with a fourth-order polynomial, which contains 15 parameters and optionally an additional parameter for Hartree–Fock exchange. The parameters were determined by minimizing the sum of the squared deviation of the energy differences calculated at the MC-DCFT level from the accurate energy differences for all 119 data points in the database:

$$\sum_{i=1}^{119} |\Delta E_i(\text{MC-DCFT}) - \Delta E_i(\text{accurate})|^2$$
(9)

To test a variety of possibilities, we optimized three versions of the density coherence functional:

- rcHCTH: reparametrized converted HCTH functional.
 This is an MC-DCFT functional converted from the HCTH functional form with all 15 parameters reoptimized.
- rcHCTH0: hybrid reparametrized converted HCTH functional, with parameter X set to 0.25. Except for X, the parameters in rcHCTH0 are the same as in rcHCTH. The use of suffix 0 to denote X = 0.25 follows the same convention as used for PBE0 in KS-DFT and tPBE0 in HMC-PDFT.
- rcHCTHh: hybrid reparametrized converted HCTH functional, with the parameter X optimized against the database. The suffix h denotes hybrid. The optimized value of X turns out to be \sim 0.46. In rcHCTHh, the parameters are reoptimized simultaneously with X.

Full sets of parameters are listed in the SI.

The accuracy of various methods is summarized in Table 1 by using two metrics, namely, mean unsigned error (MUE)

Table 1. Errors (kcal/mol) for Both DS1 and DS2

	Dissociation energy MUE	Barrier height MUE	DS1 MUE	DS2 MUE	Overall MUE ± SDUE	
Wave function theory						
CASSCF	15.4	12.6	15.2	13.0	14.0 ± 7.5	
CASPT2	4.9	3.2	4.1	3.9	4.0 ± 2.6	
KS-DFT						
PBE	6.7	9.7	8.1	8.3	8.2 ± 5.3	
BLYP	6.1	8.6	7.5	7.3	7.4 ± 4.8	
НСТН	5.8	5.9	5.9	5.8	5.9 ± 3.8	
MN15-L	3.2	1.4	2.3	2.3	2.3 ± 2.5	
HKS-DFT						
B97-1	3.4	4.6	4.0	4.1	4.0 ± 3.0	
MN15	2.8	1.3	2.1	2.0	2.0 ± 2.7	
MC-DCFT						
rcHCTH	4.6	3.8	3.8	4.6	4.2 ± 3.3	
HMC-DCFT						
rcHCTH0	4.1	3.3	3.7	3.7	3.7 ± 3.2	
rcHCTHh	2.0	1.8	1.8	2.0	1.9 ± 1.5	

and standard deviation from the mean of the unsigned error (SDUE). We present results by the following methods for comparison: for WFT methods, we consider CASSCF and CASPT2; for KS-DFT functionals, we consider BLYP, 61–63 HCTH/407⁶⁰ (abbreviated below and in the tables—as is usual in the literature—as HCTH), MN15-L, 64 and PBE; 65 for hybrid KS-DFT (HKS-DFT), we consider B97-1⁵⁹ and MN15. 66 Note that MN15-L and MN15 are trained on the Minnesota database, which includes the databases used in this study. HCTH training included some of the bond dissociation energies that are present in our databases, but its training set is very different. In Table 1, we compare the accuracy for both DS1 and DS2, where all 119 data points in both databases are assigned equal weights when computing the overall MUE and SDUE.

As shown in Table 1, all three new functionals significantly outperform CASSCF, and both hybrid functionals outperform CASPT2. All three functionals have improved accuracy compared to four of the seven KS-DFT functionals, and the fully optimized new functional, rcHCTHh, even outperforms the best of the KS-DFT functionals in terms of overall error. When we consider the many years of effort that went into optimizing KS-DFT functionals and that this is a first attempt at broad parametrization of a DCFT functional, the results are even more impressive.

When we specifically compare rcHCTHh to its KS-DFT counterpart functionals, which are HCTH and B97-1 (note that B97-1 is essentially a hybrid version of HCTH), we see the errors decrease by factors of three and two, respectively. Not only does rcHCTHh have the lowest MUE among all the methods considered, but also it has good performance for both dissociation energy and barrier heights. By comparing the standard deviation of the unsigned error in Table 1, as well as the error distribution by a histogram of mean unsigned error across various methods (Figures S2 and S3 in the SI), we see that rcHCTHh not only has the lowest MUE, but the unsigned errors of the individual data points also have the lowest deviation from the MUE.

Since *Molpro* does not have the capability of running MC-PDFT calculations, we can only compare to MC-PDFT for DS2; we do this in Table 2, where we also include the accuracy

Table 2. Errors (kcal/mol) for DS2 Only

	Dissociation energy MUE	Barrier height MUE	DS2 MUE ± SDUE				
Wave function theory							
CASSCF	13.5	12.6	13.0 ± 7.2				
CASPT2	4.8	3.0	3.9 ± 2.6				
KS-DFT							
PBE	6.7	10.0	8.3 ± 5.0				
BLYP	5.8	8.8	7.3 ± 4.6				
HCTH	5.5	6.2	5.8 ± 3.6				
MN15-L	3.2	1.5	2.3 ± 2.5				
HKS-DFT							
B97-1	3.4	4.8	4.1 ± 2.9				
MN15	2.7	1.3	2.0 ± 2.8				
MC-PDFT							
tBLYP	7.9	3.0	5.4 ± 4.4				
tPBE	4.3	3.5	3.9 ± 3.3				
HMC-PDFT							
tPBE0	5.0	2.0	3.5 ± 2.8				
MC-DCFT							
rcHCTH	5.2	4.0	4.6 ± 3.7				
HMC-DCFT							
rcHCTH0	4.4	3.0	3.7 ± 3.4				
rcHCTHh	2.3	1.7	2.0 ± 1.7				

of three MC-PDFT and HMC-PDFT methods, namely, tPBE, tBLYP, and tPBE0. Note that none of these three functionals are parametrized against DS2, and the tPBE functional is translated from the PBE functional with no additional parametrization. The table shows that the tPBE0 functional of MC-PDFT has an MUE 1.7 times larger than that of the new rcHCTHh functional, and tBLYP and tPBE have even larger MUEs.

To demonstrate that the functional still needs improvement, we calculated the potential energy curve of N_2 using rcHCTHh with the same active space and basis set as used for bond energy calculations. The result is given in Figure 1. Although the N_2 dissociation energy is part of the training data, no potential curves were used for parameter optimization. The figure shows that the rcHCTHh, PBE0, and experimental 67

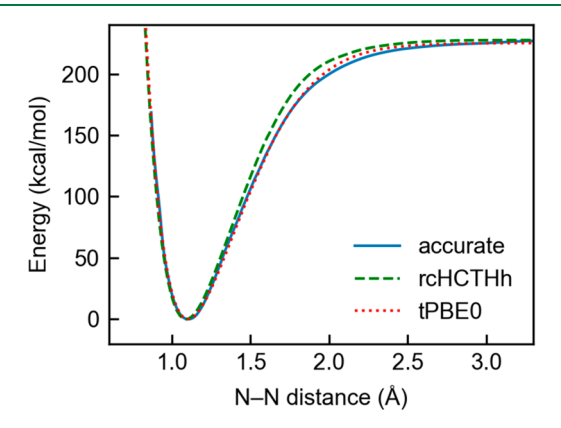


Figure 1. Potential energy curve of N_2 at rcHCTHh and tPBE0 levels compared to the accurate curve. ⁶⁷ The active space has 10 active electrons in 10 active orbitals, and the ma-TZVP basis set ^{68,69} is used.

curves agree well with each other on the repulsive well and near equilibrium, but the difference is larger between 2.0 and 2.5 Å. Both rcHCTHh and tPBE0 overestimate the energy in this region, with the rcHCTHh curve having a larger deviation from the accurate curve. The experimental curve has an estimated error of less than 0.02 eV (~0.5 kcal/mol) at shorter bond distances (~1.7 Å) and an estimated error of less than 0.2 eV (~5 kcal/mol) in other regions.⁶⁷ The energy overestimations of rcHCTHh and tPBE0 dissociation curves are larger than the uncertainty of the experimental curve. We found a similar overestimation of the energy at intermediate geometries in dissociation curves in our previous work.³⁹ This shows that more work is needed to improve the accuracy of the density coherence functional, as might be expected since the present parametrization set contains only bond energies and barrier heights.

We have presented our initial effort on developing a more broadly accurate density coherence functional through parametrization over a diverse database; the database contains 119 bond dissociation energies and reaction barrier heights. This study reveals the potential of the HMC-DCFT theoretical framework to achieve high accuracy while maintaining low computational costs. The new functional, rcHCTHh, has an overall mean unsigned error of 1.9 kcal/mol over the entire database, which outperforms all other computational methods tested, including modern Kohn-Sham functionals, three of our previously developed MC-PDFT functionals, and the much more expensive CASPT2 method. This shows that HMC-DCFT is a promising electronic structure method. However, we recognize that further optimization on an even more diverse data set is required to provide a more universal functional.

ASSOCIATED CONTENT

Supporting Information

The Supporting Information is available free of charge at https://pubs.acs.org/doi/10.1021/acs.jctc.3c00741.

Computational details, optimized parameters, smoothness test, histograms of unsigned errors, and energies of the calculations on the databases (PDF)

AUTHOR INFORMATION

Corresponding Author

Donald G. Truhlar – Department of Chemistry, Chemical Theory Center, and Minnesota Supercomputing Institute, University of Minnesota, Minneapolis, Minnesota 55455-0431, United States; orcid.org/0000-0002-7742-7294; Email: truhlar@umn.edu

Author

Dayou Zhang — Department of Chemistry, Chemical Theory Center, and Minnesota Supercomputing Institute, University of Minnesota, Minneapolis, Minnesota 55455-0431, United States; orcid.org/0000-0002-5393-657X

Complete contact information is available at: https://pubs.acs.org/10.1021/acs.jctc.3c00741

Notes

The authors declare no competing financial interest.

ACKNOWLEDGMENTS

We are grateful to Siriluk Kanchanakungwankul for helpful assistance and Laura Gagliardi for valuable cooperation. This research was supported in part by the National Science Foundation under grant CHE-2054723.

REFERENCES

- (1) Buenker, R. J.; Peyerimhoff, S. D. Energy Extrapolation in CI Calculations. *Theor. Chim. Acta* 1975, 39, 217–228.
- (2) Čársky, P.; Bartlett, R. J.; Fitzgerald, G.; Noga, J.; Špirko, V. Ab Initio Calculations on the Energy of Activation and Tunneling in the Automerization of Cyclobutadiene. *J. Chem. Phys.* **1988**, *89*, 3008–3015.
- (3) Andersson, K.; Malmqvist, P.; Roos, B. O. Second-order Perturbation Theory with a Complete Active Space Self-Consistent Field Reference Function. *J. Chem. Phys.* **1992**, *96*, 1218–1226.
- (4) Hirao, K. Multireference Møller-Plesset Method. Chem. Phys. Lett. 1992, 190, 374-380.
- (5) Lindh, R.; Persson, B. J. Ab initio study of the Bergman Reaction: The Autoaromatization of Hex-3-ene-1,5-diyne. *J. Am. Chem. Soc.* **1994**, *116*, 4963–4969.
- (6) Szalay, P. G.; Bartlett, R. J. Approximately Extensive Modifications of the Multireference Configuration Interaction Method: A Theoretical and Practical Analysis. *J. Chem. Phys.* **1995**, 103, 3600–3612.
- (7) Cramer, C. J.; Smith, B. A.; Tolman, W. B. Ab Initio Characterization of the Isomerism Between the μ - η^2 : η^2 -Peroxoand Bis(μ -oxo)dicopper Cores. *J. Am. Chem. Soc.* **1996**, *118*, 11283–11287.
- (8) Werner, H.-J. Third-order Multireference Perturbation Theory: The CASPT3Method. *Mol. Phys.* **1996**, *89*, 645–661.
- (9) Schmidt, M. W.; Gordon, M. S. The Construction and Interpretation of MCSCF Wavefunctions. *Annu. Rev. Phys. Chem.* **1998**, 49, 233–266.
- (10) Nakao, Y.; Taketsugu, T.; Hirao, K. Theoretical Study of Ammonia Activation by M^+ (M = Sc, Ni, Cu). *J. Chem. Phys.* **1999**, 110, 10863–10873.
- (11) Shavitt, I. Multi-State Multireference Rayleigh-Schrödinger Perturbation Theory for Mixed Electronic States: Second and Third Order. *Int. J. Mol. Sci.* **2002**, *3*, 639–655.
- (12) Hachmann, J.; Cardoen, W.; Chan, G. K.-L. Multireference Correlation in Long Molecules with the Quadratic Scaling Density Matrix Renormalization Group. *J. Chem. Phys.* **2006**, *125*, No. 144101.
- (13) Piecuch, P.; Włoch, M.; Varandas, A. J. C. Application of Renormalized Coupled-Cluster Methods to Potential Function of Water. *Theor. Chem. Acc.* **2008**, *120*, 59–78.
- (14) Chen, H.; Song, J.; Lai, W.; Wu, W.; Shaik, S. Multiple Low-Lying States for Compound I of P450cam and Chloroperoxidase Revealed from Multireference Ab Initio QM/MM Calculations. *J. Chem. Theory Comput.* **2010**, *6*, 940–953.
- (15) Wu, W.; Su, P.; Shaik, S.; Hiberty, P. C. Classical Valence Bond Approach by Modern Methods. *Chem. Sci.* **2011**, *111*, 7557–7593.
- (16) Shamasundar, K. R.; Knizia, G.; Werner, H.-J. A New Internally Contracted Multi-Reference Configuration Interaction Method. *J. Chem. Phys.* **2011**, *135*, No. 054101.
- (17) Szalay, P. G.; Müller, T.; Gidofalvi, G.; Lischka, H.; Shepard, R. Multiconfiguration Self-Consistent Field and Multireference Configuration Interaction Methods and Applications. *Chem. Rev.* **2012**, *112*, 108–181.
- (18) Atanasov, M.; Zadrozny, J. M.; Long, J. R.; Neese, F. (A Theoretical Analysis of Chemical Bonding, Vibronic Coupling, and Magnetic Anisotropy in Linear Iron(II) Complexes with Single-Molecule Magnet Behavior. *Chem. Sci.* 2013, 4, 139–156.
- (19) Keller, S.; Boguslawski, K.; Janowski, T.; Reiher, M.; Pulay, P. Selection of Active Spaces for Multiconfigurational Wavefunctions. *J. Chem. Phys.* **2015**, *142*, No. 244104.

- (20) Dawes, R.; Ndengué, S. A. Single- and Multireference Electronic Structure Calculations for Constructing Potential Energy Surfaces. *Int. Rev. Phys. Chem.* **2016**, *35*, 441–478.
- (21) Lischka, H.; Nachtigallová, D.; Aquino, A. J. A.; Szalay, P. G.; Plasser, F.; Machado, F. B. C.; Barbatti, M. Multireference Approaches for Excited States of Molecules. *Chem. Rev.* **2018**, *118*, 7293–7361.
- (22) Mato, J.; Gordon, M. S. Analytic Gradients for the Spin-Flip ORMAS-CI Method: Optimizing Minima, Saddle Points, and Conical Intersections. *J. Phys. Chem. A* **2019**, *123*, 1260–1272.
- (23) Zanchet, A.; López-Caballero, P.; Mitrushchenkov, A. O.; Buceta, D.; López-Quintela, M. A.; Hauser, A. W.; Pilar De Lara-Castells, M. On the Stability of Cu_5 Catalysts in Air Using Multireference Perturbation theory. J. Phys. Chem. C 2019, 123, 27064–27072.
- (24) Wu, C.-H.; Magers, D. B.; Harding, L. B.; Klippenstein, S. J.; Allen, W. D. Reaction Profiles and Kinetics for Radical-Radical Hydrogen Abstraction via Multireference Coupled Cluster theory. *J. Chem. Theory Comput.* **2020**, *16*, 1511–1525.
- (25) Zuo, J.; Chen, Q.; Hu, X.; Guo, H.; Xie, D. Theoretical Investigations of Rate Coefficients for $H+O_3$ and HO_2+O Reactions on a Full-Dimensional Potential Energy Surface. *J. Phys. Chem. A* **2020**, 124, 6427–6437.
- (26) Dunning, T. H., Jr.; Xu, L. T.; Cooper, D. L.; Karadakov, P. B. Spin-Coupled Generalized Valence Bond Theory: New Perspectives on the Electronic Structure of Molecules and Chemical Bonds. *J. Phys. Chem. A* **2021**, *125*, 2021–2050.
- (27) Zheng, P.; Ji, C.; Ying, F.; Su, P.; Wu, W. A Valence-Bond-Based Multiconfigurational Density Functional Theory: The λ -DFVB Method Revisited. *Molecules* **2021**, *26*, 521.
- (28) Zhou, C.; Hermes, M. R.; Wu, D.; Bao, J. J.; Pandharkar, R.; King, D. S.; Zhang, D.; Scott, T. R.; Lykhin, A. O.; Gagliardi, L.; Truhlar, D. G. Electronic Structure of Strongly Correlated Systems: Recent Developments in Multiconfiguration Pair-Density Functional Theory and Multiconfiguration Nonclassical-Energy Functional Theory. *Chem. Sci.* 2022, *13*, 7685–7706.
- (29) Zheng, P.; Gan, Z.; Zhou, C.; Su, P.; Wu, W. λ-DFVB(U): A Hybrid Density Functional Valence Bond Method Based on Unpaired Electron Density. *J. Chem. Phys.* **2022**, *156*, No. 204103.
- (30) Ray, D.; Oakley, M. S.; Sarkar, A.; Bai, X.; Gagliardi, L. Theoretical Investigation of Single-Molecule-Magnet Behavior in Mononuclear Dysprosium and Californium Complexes. *Inorg.Chem.* **2023**, *62*, 1649–1658.
- (31) Roos, B. O.; Taylor, P. R.; Siegbahn, P. E. M. A Complete Active Space SCF Method (CASSCF) Using a Density Matrix Formulated Super-CI Approach. *Chem. Phys.* **1980**, 48, 157–173.
- (32) Ruedenberg, K.; Schmidt, M. W.; Gilbert, M. M.; Elbert, S. T. Are Atoms Intrinsic to Molecular Wave Functions? I. The FORS Model. *Chem. Phys.* **1982**, *71*, 41–49.
- (33) Zgid, D.; Nooijen, M. The Density Matrix Renormalization Group Self-Consistent Field Method: Orbital Optimization with the Density Matrix Renormalization Group Method in the Active Space. *J. Chem. Phys.* **2008**, *128*, No. 144116.
- (34) Ghosh, D.; Hachmann, J.; Yanai, T.; Chan, G. K.-L. Orbital Optimization in the Density Matrix Renormalization Group, with Applications to Polyenes and β -Carotene. *J. Chem. Phys.* **2008**, *128*, No. 144117.
- (35) Kurashige, Y.; Yanai, T. Second-Order Perturbation Theory with a Density Matrix Renormalization Group Self-Consistent Field Reference Function: Theory and Application to the Study of Chromium Dimer. *J. Chem. Phys.* **2011**, *135*, No. 094104.
- (36) Li Manni, G.; Carlson, R. K.; Luo, S.; Ma, D.; Olsen, J.; Truhlar, D. G.; Gagliardi, L. Multiconfiguration Pair-Density Functional Theory. *J. Chem. Theory Comput.* **2014**, *10*, 3669–3680.
- (37) Gagliardi, L.; Truhlar, D. G.; Li Manni, G.; Carlson, R. K.; Hoyer, C. E.; Bao, J. L. Multiconfiguration Pair-Density Functional Theory: A New Way to Treat Strongly Correlated Systems. *Acc. Chem. Res.* **2017**, *50*, 66–73.

- (38) King, D. S.; Truhlar, D. G.; Gagliardi, L. Machine-Learned Energy Functionals for Multiconfigurational Wave Functions. *J. Phys. Chem. Lett.* **2021**, *12*, 7761–7767.
- (39) Zhang, D.; Hermes, M. R.; Gagliardi, L.; Truhlar, D. G. Multiconfiguration Density-Coherence Functional Theory. *J. Chem. Theory Comput.* **2021**, *17*, 2775–2782.
- (40) Kohn, W.; Sham, L. J. Self-Consistent Equations Including Exchange and Correlation Effects. *Phys. Rev.* **1965**, *140*, A1133–A1138.
- (41) Pople, J. A.; Gill, P. M. W.; Handy, N. C. Spin-Unrestricted Character of Kohn-Sham Orbitals for Open-She11 Systems. *Int. J. Quantum Chem.* **1995**, *56*, 303–305.
- (42) Zhang, D.; Truhlar, D. G. Decomposition of the Electronic Energy in Terms of Density, Density Coherence, and the Connected Part of the Two-Body Reduced Density Matrix. *J. Chem. Theory Comput.* **2021**, *17*, 5733–5744.
- (43) Stroscio, G.; Zhou, C.; Truhlar, D. G.; Gagliardi, L. Multiconfiguration Pair-Density Functional Theory Calculations of Iron(II) Porphyrin: Effects of Hybrid Pair-Density Functionals and Expanded RAS and DMRG Active Spaces on Spin-State Orderings. *J. Phys. Chem. A* 2022, 126, 3957–3963.
- (44) Sauza-de la Vega, A.; Pandharkar, R.; Stroscio, G. D.; Sarkar, A.; Truhlar, D. G.; Gagliardi, L. Multiconfiguration Pair-Density Functional Theory for Chromium(IV) Molecular Qubits. *JACS Au* **2022**, *2*, 2029–2037.
- (45) Zhang, P.; Nabi, R.; Staab, J. K.; Chilton, N. F.; Demir, S. Taming Super-Reduced Bi23—Radicals with Rare Earth Cations. *J. Am. Chem. Soc.* **2023**, *145*, 9152—9163.
- (46) Pandharkar, R.; Hermes, M. R.; Truhlar, D. G.; Gagliardi, L. A New Mixing of Nonlocal Exchange and Nonlocal Correlation with Multiconfiguration Pair-Density Functional Theory. *J. Phys. Chem. Lett.* **2020**, *11*, 10158–10163.
- (47) Lykhin, A. O.; Truhlar, D. G.; Gagliardi, L. Dipole Moment Calculations Using Multiconfiguration Pair-Density Functional Theory and Hybrid Multiconfiguration Pair-Density Functional Theory. J. Chem. Theory Comput. 2021, 17, 7586–7601.
- (48) King, D. S.; Hermes, M. R.; Truhlar, D. G.; Gagliardi, L. Large-Scale Benchmarking of Multireference Vertical-Excitation Calculations via Automated Active-Space Selection. *J. Chem. Theory Comput.* **2022**, *18*, 6065–6076.
- (49) Takatsuka, K.; Fueno, T.; Yamaguchi, K. Distribution of Odd Electrons in Ground-State Molecules. *Theor. Chim. Acta* **1978**, 48, 175–183.
- (50) Staroverov, V. N.; Davidson, E. R. Diradical Character of the Cope Rearrangement Transition State. *J. Am. Chem. Soc.* **2000**, *122*, 186–187.
- (51) Staroverov, V. N.; Davidson, E. R. Distribution of Effectively Unpaired Electrons. *Chem. Phys. Lett.* **2000**, 330, 161–168.
- (52) Fdez. Galván, I.; Vacher, M.; Alavi, A.; Angeli, C.; Aquilante, F.; Autschbach, J.; Bao, J. J.; Bokarev, S. I.; Bogdanov, N. A.; Carlson, R. K.; Chibotaru, L. F.; Creutzberg, J.; Dattani, N.; Delcey, M. G.; Dong, S. S.; Dreuw, A.; Freitag, L.; Frutos, L. M.; Gagliardi, L.; Gendron, F.; Giussani, A.; González, L.; Grell, G.; Guo, M.; Hoyer, C. E.; Johansson, M.; Keller, S.; Knecht, S.; Kovačević, G.; Källman, E.; Li Manni, G.; Lundberg, M.; Ma, Y.; Mai, S.; Malhado, J. P.; Malmqvist, P. Å.; Marquetand, P.; Mewes, S. A.; Norell, J.; Olivucci, M.; Oppel, M.; Phung, Q. M.; Pierloot, K.; Plasser, F.; Reiher, M.; Sand, A. M.; Schapiro, I.; Sharma, P.; Stein, C. J.; Sørensen, L. K.; Truhlar, D. G.; Ugandi, M.; Ungur, L.; Valentini, A.; Vancoillie, S.; Veryazov, V.; Weser, O.; Wesołowski, T. A.; Widmark, P.; Wouters, S.; Zech, A.; Zobel, J. P.; Lindh, R. OpenMolcas: From Source Code to Insight. J. Chem. Theory Comput. 2019, 15, 5925–5964.
- (53) Werner, H.-J.; Knowles, P. J.; Knizia, G.; Manby, F. R.; Schütz, M.; Celani, P.; Korona, T.; Lindh, R.; Mitrushenkov, A.; Rauhut, G.; Shamasundar, K. R.; Adler, T. B.; Amos, R. D.; Bernhardsson, A.; Berning, A.; Cooper, D. L.; Deegan, M. J. O.; Dobbyn, A. J.; Eckert, F.; Goll, E.; Hampel, C.; Hesselmann, A.; Hetzer, G.; Hrenar, T.; Jansen, G.; Köppl, C.; Liu, Y.; Lloyd, A. W.; Mata, R. A.; May, A. J.; Mcnicholas, S. J.; Meyer, W.; Mura, M. E.; Nicklass, A.; O'Neill, D. P.;

- Palmieri, P.; Peng, D.; Pflüger, K.; Pitzer, R.; Reiher, M.; Shiozaki, T.; Stoll, H.; Stone, A. J.; Tarroni, R.; Thorsteinsson, T.; Wang, M.; Welborn, M.; Ziegler, B. *Molpro, version 2019.2, A package of ab initio programs*; http://www.molpro.net (accessed 2023-06-22).
- (54) Werner, H.; Knowles, P. J.; Knizia, G.; Manby, F. R.; Schütz, M. Molpro: A General-Purpose Quantum Chemistry Program Package. *Wiley Interdiscip. Rev. Comput. Mol. Sci.* **2012**, 2 (2), 242–253.
- (55) Werner, H.; Knowles, P. J.; Manby, F. R.; Black, J. A.; Doll, K.; Heßelmann, A.; Kats, D.; Köhn, A.; Korona, T.; Kreplin, D. A.; Ma, Q.; Miller, T. F.; Mitrushchenkov, A.; Peterson, K. A.; Polyak, I.; Rauhut, G.; Sibaev, M. The Molpro Quantum Chemistry Package. *J. Chem. Phys.* **2020**, *152*, No. 144107.
- (56) Bao, J. L.; Odoh, S. O.; Gagliardi, L.; Truhlar, D. G. Predicting Bond Dissociation Energies of Transition-Metal Compounds by Multiconfiguration Pair-Density Functional Theory and Second-Order Perturbation Theory Based on Correlated Participating Orbitals and Separated Pairs. *J. Chem. Theory Comput.* **2017**, *13*, 616–626.
- (57) Verma, P.; Truhlar, D. G. Geometries for Minnesota Database 2019; Retrieved from the Data Repository for the University of Minnesota, 2019. https://doi.org/10.13020/217y-8g32 (accessed 2023-09-01).
- (58) Becke, A. D. Density-Functional Thermochemistry. V. Systematic Optimization of Exchange-Correlation Functionals. *J. Chem. Phys.* **1997**, *107*, 8554–8560.
- (59) Hamprecht, F. A.; Cohen, A. J.; Tozer, D. J.; Handy, N. C. Development and Assessment of New Exchange-Correlation Functionals. *J. Chem. Phys.* **1998**, *109*, 6264–6271.
- (60) Boese, A. D.; Handy, N. C. A New Parametrization of Exchange-correlation Generalized Gradient Approximation Functionals. *J. Chem. Phys.* **2001**, *114*, 5497–5503.
- (61) Becke, A. D. Density-Functional Exchange-Energy Approximation with Correct Asymptotic Behavior. *Phys. Rev. A* **1988**, 38, 3098–3100.
- (62) Lee, C.; Yang, W.; Parr, R. G. Development of the Colle-Salvetti Correlation-Energy Formula into a Functional of the Electron Density. *Phys. Rev. B* **1988**, *37*, 785–789.
- (63) Miehlich, B.; Savin, A.; Stoll, H.; Preuss, H. Results Obtained with the Correlation Energy Density Functionals of Becke and Lee, Yang and Parr. *Chem. Phys. Lett.* **1989**, *157*, 200–206.
- (64) Yu, H. S.; He, X.; Truhlar, D. G. MN15-L: A New Local Exchange-Correlation Functional for Kohn—Sham Density Functional Theory with Broad Accuracy for Atoms, Molecules, and Solids. *J. Chem. Theory Comput.* **2016**, *12*, 1280—1293.
- (65) Perdew, J. P.; Burke, K.; Ernzerhof, M. Generalized Gradient Approximation Made Simple. *Phys. Rev. Lett.* **1996**, 77, 3865–3868.
- (66) Yu, H. S.; He, X.; Li, S. L.; Truhlar, D. G. MN15: A Kohn–Sham Global-Hybrid Exchange–correlation Density Functional with Broad Accuracy for Multi-Reference and Single-Reference Systems and Noncovalent Interactions. *Chem. Sci.* **2016**, *7*, 5032–5051.
- (67) Gilmore, F. R. Potential Energy Curves for N₂, NO, O₂ and Corresponding Ions. *J. Quant. Spectrosc. Radiat. Transfer* **1965**, 5, 369–IN3.
- (68) Weigend, F.; Ahlrichs, R. Balanced Basis Sets of Split Valence, Triple Zeta Valence and Quadruple Zeta Valence Quality for H to Rn: Design and Assessment of Accuracy. *Phys. Chem. Chem. Phys.* **2005**, *7*, 3297.
- (69) Zheng, J.; Xu, X.; Truhlar, D. G. Minimally Augmented Karlsruhe Basis Sets. *Theor. Chem. Acc.* **2011**, *128*, 295–305.